J|A|C|S ARTICLES

Published on Web 08/30/2010

Charge-Transfer Energy in the Water−Hydrogen Molecular Aggregate Revealed by Molecular-Beam Scattering Experiments, Charge Displacement Analysis, and ab Initio Calculations

Leonardo Belpassi,[*,†,‡] Michael L. Reca,[†] Francesco Tarantelli,[*,†,‡] Luiz F. Roncaratti,[†,⊥] Fernando Pirani,[*,†] David Cappelletti,[*,¶] Alexandre Faure,[§] and Yohann Scribano[||]

Dipartimento di Chimica, Università di Perugia, and CNR−Istituto di Scienze e Tecnologie Molecolari, Via Elce di Sotto 8, 06123 Perugia, Italy, Dipartimento di Ingegneria Civile e Ambientale, Università di Perugia, Via G. Duranti 93, 06125 Perugia, Italy, Laboratoire d'Astrophysique, Observatoire de Grenoble, Université Joseph Fourier, CNRS UMR5571, B.P. 53, 38041 Grenoble Cedex 09, France, and Laboratoire Interdisciplinaire Carnot de Bourgogne, UMR 5209 CNRS−Université de Bourgogne, 9 Avenue Alain Savary, B.P. 47870, F-21078 Dijon Cedex, France

Received June 28, 2010; E-mail: belp@thch.unipg.it; franc@thch.unipg.it; pirani@dyn.unipg.it; david.cappelletti@unipg.it

Abstract: Integral cross-section measurements for the system water−H_2 in molecular-beam scattering experiments are reported. Their analysis demonstrates that the average attractive component of the water−H_2 intermolecular potential in the well region is about 30% stronger than dispersion and induction forces would imply. An extensive and detailed theoretical analysis of the electron charge displacement accompanying the interaction, over several crucial sections of the potential energy surface (PES), shows that water−H_2 interaction is accompanied by charge transfer (CT) and that the observed stabilization energy correlates quantitatively with CT magnitude at all distances. Based on the experimentally determined potential and the calculated CT, a general theoretical model is devised which reproduces very accurately PES sections obtained at the CCSD(T) level with large basis sets. The energy stabilization associated with CT is calculated to be 2.5 eV per electron transferred. Thus, CT is shown to be a significant, strongly stereospecific component of the interaction, with water functioning as electron donor or acceptor in different orientations. The general relevance of these findings for water's chemistry is discussed.

Introduction

The study of static and dynamic properties of aggregates formed by water with neutral and ionic species, and with electrons, is of great importance in order to understand and control several elementary processes occurring in condensed and gas phases and at interfaces (see for example ref 1). The present paper focuses on the detailed experimental and theoretical investigation of the nature of the H_2O-H_2 intermolecular potential, with crucial results concerning the assessment of the stereoselectivity of the leading interaction components. The water−hydrogen molecular aggregate is the simplest example of noncovalent interaction between water and other molecules. This complex is important in science. First, while H_2 is by far the most abundant molecule in the interstellar clouds, water, although ubiquitous, is much less abundant ($[H_2O]/[H_2] < 10^{-4}$). Therefore, the possibility of formation and the role of a stable (or metastable) H_2O-H_2 complex are open fundamental questions. In any case, due to the coexistence of H_2O and H_2 in interstellar molecular clouds, several rotational and vibrational transitions of water perturbed by hydrogen have been detected, including various maser lines. Masers are generated effectively in star-forming regions, where water plays a central role in the chemistry and cooling of molecular gas during the protostellar collapse.[2] We note that water is a prime target of the Herschel

[†] Dipartimento di Chimica, Università di Perugia.
[‡] CNR−ISTM, Perugia.
[¶] Dipartimento di Ingegneria Civile e Ambientale, Università di Perugia.
[§] Laboratoire d'Astrophysique, Université Joseph Fourier.
[||] Laboratoire Interdisciplinaire Carnot de Bourgogne, Université de Bourgogne.
[⊥] Permanent address: Instituto de Física, Universidade de Brasília, 04455 Brasília, Brazil.

(1) (a) Siefermann, K. R.; Liu, Y.; Lugovoy, E.; Link, O.; Faubel, M.; Buck, U.; Winter, B.; Abel, B. *Nature Chem.* **2010**, *2*, 274–279. (b) Klemperer, W.; Vaida, V. *Proc. Natl. Acad. Sci. U.S.A.* **2006**, *103*, 10584–10588.

(2) (a) Bergin, E.; et al. *Astrophys. J.* **2000**, *539*, L129–L132. (b) Tereszchuk, K.; Bernath, P. F.; Zobov, N. F.; Shirin, S. V.; Polyansky, O. L.; Libeskind, N. I.; Tennyson, J.; Wallace, L. *Astrophys. J.* **2002**, *577*, 496. (c) Hagiwara, Y.; Diamond, P. J.; Miyoshi, M. *Astron. Astrophys.* **2003**, *400*, 457–463. (d) Furuya, R.; Kitamura, Y.; Wootten, A.; Claussen, M.; Kawabe, R. *Astrophys. J. Suppl. S* **2003**, *144*, 71–134. (e) Neufeld, D. A.; Bergin, E. A.; Melnick, G. J.; Goldsmith, P. F. *Astrophys. J.* **2003**, *590*, 882. (f) Cernicharo, J.; Goicoechea, J. R.; Daniel, F.; Lerate, M. R.; Barlow, M. J.; Swinyard, B. M.; van Dishoeck, E. F.; Lim, T. L.; Viti, S.; Yates, J. *Astrophys. J.* **2006**, *649*, L33–L36.

 10.1021/ja1056642

Space Observatory, which was launched in May 2009.[3] Herschel will observe H_2O lines, including ^{17}O, ^{18}O, and D isotopologues, in regimes from the cold interstellar medium to stellar, planetary, and cometary atmospheres, with unprecedented sensitivity and spectral resolution. The detailed interpretation of these spectra will depend critically on the accuracy of the available molecular data.

Theoretical studies of spectral line formation predict that the observed intensities depend on a complex balance between radiative and collision excitation processes.[4] Therefore, a meaningful analysis of these data involves an accurate description of state-to-state collisional excitation rates based on a detailed knowledge of the intermolecular interaction, coupled with a proper treatment of the collisional dynamics.

The water−hydrogen interaction is also crucial for predicting thermodynamics and transport properties of gaseous mixtures related to combustion processes and for certain types of fuel cells. Furthermore, the stability of molecular hydrogen in clatrate hydrate structure is of great importance for hydrogen storage.[5] Finally, the investigation of H_2 in liquid water and absorbed in amorphous ice is also of great interest (see for example ref 6).

To our knowledge, characterizations of the potential energy surface (PES) for H_2O-H_2 by various quantum-chemical methods began to appear in the literature in 1973.[7] The complexity, quality, and degree of convergence of the calculations increased over the years and are continuously being improved;[8−11] recently, a representation of the PES by an expansion in hyperspherical harmonics has been suggested.[12] On the other side, detailed tests performed on experimental observables directly affected by the strength of the intermolecular potentials are scarce. We mention in particular two important experiments: a crossed molecular-beam study, where a diffraction structure was observed in the total differential cross section,[13,14] and a spectroscopic investigation where rotovibrational bands were measured under high-resolution conditions.[14]

Herein, we report measurements of the integral cross section $Q(v)$ for the scattering of water by hydrogen molecules as a function of the collision velocity, v. The experimental conditions adopted have permitted the clear observation of an oscillatory pattern, associated with the glory quantum interference effect, superimposed to a smooth average cross-section component. These contributions depend on the absolute scale of the intermolecular interaction in the well region and at long range, respectively.[15] Since molecular beams are rotationally hot, for the analysis of $Q(v)$ we used a recently proposed isotropic model potential that involves two parameters and allows us to describe in a unifying and internally consistent way both the asymptotic region of the attraction component and the potential well.[15] It is important and instrumental to the present work to mention that this potential model has proved suitable to describe in detail not only the behavior of prototypical weakly interacting aggregates such as noble-gas dimers but also that of more strongly bound systems where ions are involved.[15] The present experimental data have also been compared with the cross section calculated using the most recently proposed theoretical PESs.[9−11] A rigid-rotor (five-dimensional) PES has been specifically obtained for the D_2O-D_2 isotopologue, starting from the flexible, nine-dimensional H_2O-H_2 PES reported by Valiron et al.,[11] accounting for the different intramolecular averaged geometries and for the shift of the D_2O center-of-mass (c.m.) with respect to H_2O.[16]

A crucial result of the present work is that the potential parameters obtained from the best fit of the experimental data differ substantially from those expected assuming that the (rotationally averaged) interaction is due to van der Waals (vdW) forces (size repulsion plus dispersion attraction) plus induction. (Note that averaging over all the possible relative molecular orientations averages out any electrostatic contribution to the potential.) In particular, our findings reveal the presence of an additional interaction component that perceptibly stabilizes at least some orientations of the water−hydrogen complex. We have thus carried out a very accurate analysis of the electron density changes accompanying the water−H_2 interaction, and we have quantitatively related the results to the computed PES. This shows without doubt that, as already found in the case of water−heavier-rare-gas complexes,[17,18] the observed stabilization component arises from charge transfer (CT). In some orientations of the adduct, a net electron transfer occurs from hydrogen to water, while in others a reverse water-to-hydrogen transfer takes place, and in yet other geometries no CT is observed. As a result, CT modulates the interaction anisotropy in a complex way but with an overall stabilizing effect. Indeed, for these reasons one can expect the CT to be crucial in determining the collision dynamics of the system, promoting the rotational inelasticity of water in the presence of hydrogen, and affecting the thermodynamic properties of their gaseous mixtures. Finally, we have studied the decay properties of CT

(3) Nisini, B.; et al. *Astron. Astrophys.* **2010**, *518*, L120.
(4) (a) Dubernet, M.-L.; Daniel, F.; Grosjean, A.; Faure, A.; Valiron, P.; Wernli, M.; Wiesenfeld, L.; Rist, C.; Noga, J.; Tennyson, J. *Astron. Astrophys.* **2006**, *460*, 323–329. (b) Faure, A.; Crimier, N.; Ceccarelli, C.; Valiron, P.; Wiesenfeld, L.; Dubernet, M. L. *Astron. Astrophys.* **2007**, *472*, 1029–1035. (c) Faure, A.; Josselin, E. *Astron. Astrophys.* **2008**, *492*, 257–264. (d) Dubernet, M.; Daniel, F.; Grosjean, A.; Lin, C. Y. *Astron. Astrophys.* **2009**, *497*, 911–925.
(5) (a) Mao, W. L.; Mao, H.-k.; Goncharov, A. F.; Struzhkin, V. V.; Guo, Q.; Hu, J.; Shu, J.; Hemley, R. J.; Somayazulu, M.; Zhao, Y. *Science* **2002**, *297*, 2247–2249. (b) Mao, W. L.; Mao, H.-k. *Proc. Natl. Acad. Sci. U.S.A.* **2004**, *101*, 708–710. (c) Sebastianelli, F.; Xu, M.; Elmatad, Y. S.; Moskowitz, J. W.; Bacic, Z. *J. Phys. Chem. C* **2007**, *111*, 2497–2504.
(6) (a) Taylor, D. G.; Strauss, H. L. *J. Chem. Phys.* **1989**, *90*, 768–772. (b) Hixson, H. G.; Wojcik, M. J.; Devlin, M. S.; Devlin, J. P.; Buch, V. *J. Chem. Phys.* **1992**, *97*, 753–767.
(7) Lischka, H. *Chem. Phys.* **1973**, *2*, 191–202.
(8) (a) Schwenke, D. W.; Walch, S. P.; Taylor, P. R. *J. Chem. Phys.* **1991**, *94*, 2986–2999. (b) Zhang, Q.; Chenyang, L.; Ma, Y.; Fish, F.; Szcześniak, M. M.; Buch, V. *J. Chem. Phys.* **1992**, *96*, 6039–6047. (c) Balasubramanian, V.; Balint-Kurti, G. G.; van Lenthe, J. H. *J. Chem. Soc., Faraday Trans.* **1993**, *89*, 2239–2253.
(9) Phillips, T. R.; Maluendes, S.; McLean, A. D.; Green, S. *J. Chem. Phys.* **1994**, *101*, 5824–5830.
(10) Hodges, M. P.; Wheatley, R. J.; Schenter, G. K.; Harvey, A. H. *J. Chem. Phys.* **2004**, *120*, 710–720.
(11) Valiron, P.; Wernli, M.; Faure, A.; Wiesenfeld, L.; Rist, C.; Kedžuch, S.; Noga, J. *J. Chem. Phys.* **2008**, *129*, 134306.
(12) Barreto, P. R. P.; Ribas, V. W.; Palazzetti, F. *J. Phys. Chem. A* **2009**, *113*, 15047–15054.
(13) Bickes, R. W., Jr.; Duquette, G.; van den Meijdenberg, C. J. N.; Rulis, A. M.; Scoles, G.; Smith, K. M. *J. Phys. B: At. Mol. Opt.* **1975**, *8*, 3034.
(14) Weida, M. J.; Nesbitt, D. J. *J. Chem. Phys.* **1999**, *110*, 156–167.
(15) Pirani, F.; Brizi, S.; Roncaratti, L. F.; Casavecchia, P.; Cappelletti, D.; Vecchiocattivi, F. *Phys. Chem. Chem. Phys.* **2008**, *10*, 5489–5503.
(16) Scribano, Y.; Faure, A.; Wiesenfeld, L., in preparation.
(17) Belpassi, L.; Tarantelli, F.; Pirani, F.; Candori, P.; Cappelletti, D. *Phys. Chem. Chem. Phys.* **2009**, *11*, 9970–9975.
(18) Roncaratti, L. F.; Belpassi, L.; Cappelletti, D.; Pirani, F.; Tarantelli, F. *J. Phys. Chem. A* **2009**, *113*, 15223–15232.

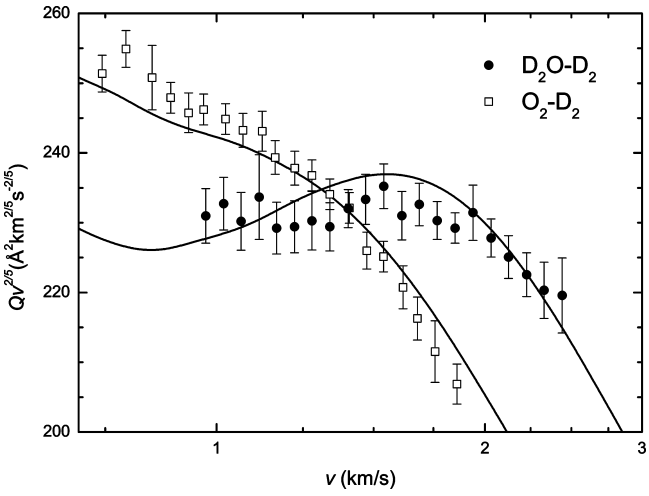

Figure 1. Cross sections Q for the D_2O-D_2 and O_2-D_2 systems as a function of the beam velocity v. Symbols are the experimental data, and lines are the fits obtained using the improved Lennard-Jones potential model.

with distance and designed a simple theoretical model to estimate its energy contribution.

Experimental Framework

The experiments have been carried out in a molecular-beam (MB) apparatus that operates under high angular and velocity resolution conditions, providing the cross section Q as a function of the collision velocity v in a range where modulation of the cross section due to the first maximum of the *glory* quantum effect is well resolved. Such an apparatus has been extensively described previously.[19] Basically, it consists of a set of differentially pumped vacuum chambers where the MB is produced by gas expansion from a nozzle heated to 550−600 K, collimated by two skimmers and one defining slit, velocity analyzed by a mechanical velocity selector (six rotating slotted disks), and attenuated by collision with a target gas contained in a scattering chamber and detected by a quadrupole mass spectrometer. The water MB is produced by using D_2O vapors at low pressure (5−6 Torr), and the scattering chamber is filled with a stationary gaseous flow of D_2. Heavy water has been employed instead of H_2O to take advantage of the smaller background signal in the mass spectrometric detector. D_2 has been chosen instead of H_2 because of the better kinematic conditions, reducing the thermal motion in the scattering box, kept at 90 K with a liquid nitrogen cryostat. The better signal-to-noise ratio and the improved velocity resolution conditions appear to be crucial to resolve the glory interference.

As before,[18,19] the water MB contains rotationally hot and randomly oriented molecules, which are scattered by the fast rotating and randomly oriented hydrogen molecules in the scattering chamber. These conditions are optimal to observe glory interference in the velocity dependence of $Q(v)$. In particular, the interaction anisotropy and the associated inelastic events play minor roles, and $Q(v)$ mostly arises from the elastic scattering driven by the rotationally averaged (isotropic) component of the interaction.[20]

Experiments have also been performed under the same conditions for an O_2 MB scattered by D_2, in order to directly compare internally consistent sets of cross-section data. The comparison between water and oxygen, in particular, is suggested by the similar value of the average molecular polarizability (1.47 and 1.60 Å^3 for water and oxygen, respectively), a quantity found to be a natural scale for both attraction and repulsion when vdW forces are involved.[21] In the case of water, a small, rotationally averaged induction effect due to its permanent dipole is also present and will be further discussed later on.

$Q(v)$ measured for the water−hydrogen and oxygen−hydrogen systems is reported in Figure 1, where the data are plotted as $Q(v) \times v^{2/5}$ in order to emphasize the interference structure. It emerges clearly from the figure that the $Q(v)$ data measured under the same conditions for the D_2O-D_2 and O_2-D_2 systems show a completely different velocity dependence pattern, although their magnitudes, averaged over the velocity range probed, appear to be very similar. These experimental findings indicate that the intermolecular potentials governing the two interactions must show very similar long-range attraction components but different strengths at intermediate intermolecular distances.

Results and Discussion

Data Analysis. We have carried out a thorough analysis of the cross-section data based on the improved Lennard-Jones (ILJ) potential model,[15,22] which reads

$$V(r) = \varepsilon\left[\frac{6}{n(r)-6}\left(\frac{r_m}{r}\right)^{n(r)} - \frac{n(r)}{n(r)-6}\left(\frac{r_m}{r}\right)^6\right] \qquad (1)$$

where

$$n(r) = \beta + 4\left(\frac{r}{r_m}\right)^2 \qquad (2)$$

In eq 1, the first term represents the repulsion and the second one the attraction. The ε parameter defines the depth of the potential well, and r_m is the equilibrium distance. In eq 2, β is a parameter related to the "hardness" of the colliding species and essentially determines the shape of the potential in the well region. As previously discussed,[15,18] we take $\beta = 9$, a value typical of weak intermolecular interactions between neutral species.[15] In this way, only the two parameters r_m and ε define the potential. These have been varied in order to reproduce the experimental cross sections, by fitting the glory extremum and the magnitude of $Q(v)$, the latter within the uncertainty of its calibration (3−4%). The cross section is calculated using the JWKB method[23] in the c.m. frame and then convoluted in the laboratory system for direct comparison with the experimental data. The convolution[19] includes the average over the thermal motion of the target gas, the transmission function of the velocity selector, and a small correction due to the finite angular resolution of the apparatus (the so-called "limit angle" correction, due to the uncertainty principle). In the O_2-D_2 case, the potential parameters obtained differ slightly (within the experimental uncertainty) from those of a previous determination carried out using a D_2 MB scattered by O_2 kept at a temperature of 90 K.[24] Figure 1 compares measured and calculated $Q(v)$. The good agreement, as in previous cases,[18,25] supports the validity of the isotropic model adopted to describe the dynamics

(19) Cappelletti, D.; Bartolomei, M.; Pirani, F.; Aquilanti, V. *J. Phys. Chem. A* **2002**, *106*, 10764–10772.
(20) Aquilanti, V.; Ascenzi, D.; Cappelletti, D.; de Castro, M.; Pirani, F. *J. Chem. Phys.* **1998**, *109*, 3898–3910.
(21) (a) Cambi, R.; Cappelletti, D.; Liuti, G.; Pirani, F. *J. Chem. Phys.* **1991**, *95*, 1852–1861. (b) Cappelletti, D.; Liuti, G.; Pirani, F. *Chem. Phys. Lett.* **1991**, *183*, 297–303.
(22) (a) Pirani, F.; Albertí, M.; Castro, A.; Moix Teixidor, M.; Cappelletti, D. *Chem. Phys. Lett.* **2004**, *394*, 37–44. (b) Candori, P.; Cappelletti, D.; Falcinelli, S.; Pirani, F.; Roncaratti, L. F.; Tarantelli, F.; Vecchiocattivi, F. *Phys. Scr.* **2008**, *78*, 038102.
(23) Child, M. S. *Molecular Collision Theory*; Academic Press: London, 1974.
(24) Aquilanti, V.; Candori, R.; Mariani, L.; Pirani, F.; Liuti, G. *J. Phys. Chem.* **1989**, *93*, 130–135.
(25) Aquilanti, V.; Cornicchi, E.; Moix Teixidor, M.; Saendig, N.; Pirani, F.; Cappelletti, D. *Angew. Chem., Int. Ed.* **2005**, *44*, 2356–2360.

Table 1. Well Depth ε and Equilibrium Distance r_m for the Spherically Averaged Interaction Obtained from the Analysis of the Present Experimental Data[a]

system	ε (meV)	r_m (Å)	source
D_2O-D_2	8.20	3.45	expt
	5.47	3.59	vdW formulas[21]
	6.46	3.55	vdW formulas[21] + induction
	7.32	3.44	theor PES[11]
H_2O-H_2	6.14	3.52	theor PES[9]
	6.62	3.42	theor PES[10]
	7.37	3.44	theor PES[11]
O_2-D_2	5.90	3.63	expt
	6.13	3.62	vdW formulas[21]
$Ar-H_2$	6.29	3.59	theor PES[26]
	6.05	3.63	vdW formulas[21]

[a] Maximum estimated uncertainty is 5% for ε and 2% for r_m. Predictions from vdW correlation formulas and from calculated PES reported in the literature are also shown for comparison. 1 meV = 0.096485 kJ mol^{-1}, and 1 Å = 0.1 nm.

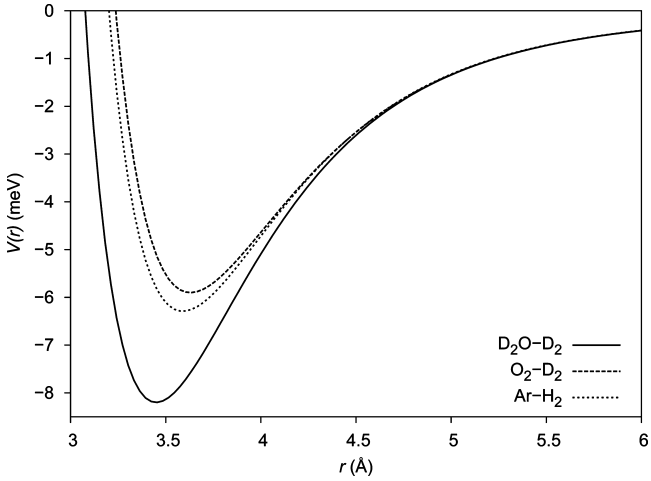

Figure 2. Experimentally determined isotropic ILJ potential energy curves for D_2O-D_2 and O_2-D_2. Also shown is a spherical average of the $Ar-H_2$ potential from ref 26.

under the present experimental conditions and confirms that the anisotropy of the electrostatic component due to the interaction of permanent multipoles plays here a marginal role, well within the experimental uncertainty.

The potential parameters derived by fitting the experimental cross-section data are reported in Table 1, and the corresponding $V(r)$ ILJ functions are plotted in Figure 2. Along with the results for D_2O-D_2 and O_2-D_2 obtained in the present work, a spherical average of the potential proposed by Bissonnette et al.[26] for the $Ar-H_2$ system is also shown. The comparison with argon is again appropriate because its polarizability (1.64 Å^3) is also very close to that of water and O_2. The figure evidences very clearly that all three potentials practically coincide for r larger than about 4.5 Å, but at shorter distances the potential for D_2O-D_2 deviates very significantly from the other two and describes the system as substantially more bound.

This finding is a key result of the present work, which confirms analogous observations made in other water MB experiments.[17,18] We must immediately dispel any doubt that the extra binding energy observed for water$-H_2$ relative to other comparable systems may be due to the induction forces arising from water's permanent dipole. The rotationally averaged

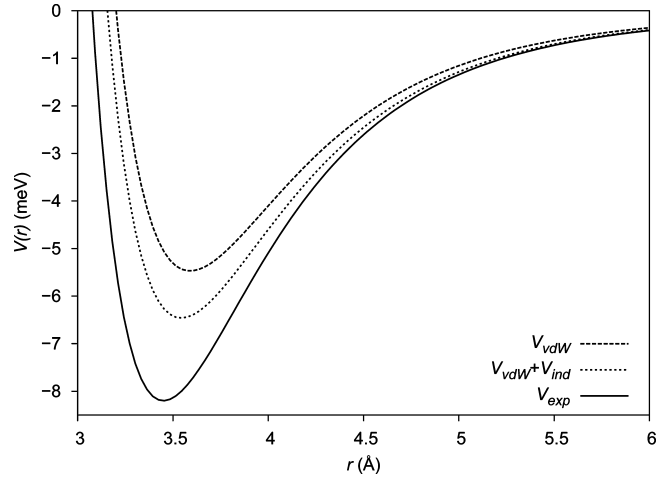

Figure 3. Comparison of the estimated van der Waals (V_{vdW}), van der Waals plus induction ($V_{vdW} + V_{ind}$), and experimentally determined potentials (V_{exp}) for water$-H_2$.

induction coefficient of the r^{-6} potential term may be estimated as[27] $\mu_w^2\alpha_{H_2}$, where μ_w is water's dipole moment (1.85 D) and α_{H_2} is hydrogen's average polarizability (0.80 Å^3). This is equal to 1.71 eV Å^6, which is only about 12% of the total long-range C_6 coefficient extracted from the ILJ potential (the latter is obtained for $r \rightarrow \infty$ as $C_6 = \varepsilon r_m^6 = 13.8$ eV Å^6). Note for comparison that, indeed, the C_6 coefficients obtained for the O_2-D_2 and $Ar-H_2$ interactions are identical (13.5 eV Å^6) and only slightly smaller than that for water. We can also confirm these conclusions regarding the magnitude of the induction effect in other ways. The r_m and ε parameters that arise from the pure vdW interaction component may be reliably estimated using empirical correlation formulas[21] that make use of the polarizabilities and effective number of valence electrons. Indeed, these provide fairly accurate approximations of the ILJ potential parameters for O_2-D_2 and the ab initio parameters for $Ar-H_2$ (see Table 1). In the case of H_2O-H_2, one thus obtains r_m = 3.59 Å and ε = 5.47 meV. Note that this potential well is in fact shallower than that of O_2-D_2 because of water's smaller polarizability. The ILJ curve corresponding to this pure vdW interaction (V_{vdW}) is shown in Figure 3. We can now write the induction attraction as $V_{ind}(r) = -C_6^{ind}/r^6$, where C_6^{ind} is taken as the difference between the experimentally determined C_6 coefficient (13.8 eV Å^6) and that obtained from V_{vdW} (11.8 eV Å^6). Note that this C_6^{ind} value is in good agreement with the semiempirical estimate given above. Adding this induction component to V_{vdW} results in the curve also shown in Figure 3, for which one obtains ε = 6.46 meV and r_m = 3.55 Å. Clearly, the attractive component of this potential is similar to those of O_2-H_2 or $Ar-H_2$ and falls far short of that determined experimentally. Note that an estimate of the induction effect essentially in agreement with the calculations above may be obtained by a simple modification of the vdW correlation formulas of ref 21. This involves increasing by about 10% the attractive factor represented by the product of the polarizabilities of the interacting molecules (see, e.g., ref 18).

In the remainder of this paper we argue that the extra stabilization energy observed for water$-H_2$ arises from charge

(26) Bissonnette, C.; Chuaqui, C. E.; Crowell, K. G.; Roy, R. J. L.; Wheatley, R. J.; Meath, W. J. *J. Chem. Phys.* **1996**, *105*, 2639–2653.

(27) Buckingham, A. D. In *Permanent and Induced Molecular Moments and Long-Range Intermolecular Forces*Hirschfelder, J. O., Ed.; Advances in Chemistry and Physics *12*; Wiley Interscience: New York, 1967; pp 107−142.

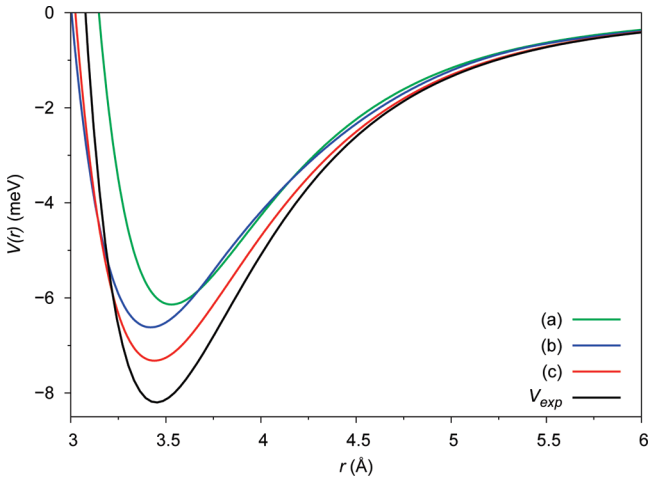

Figure 4. Spherical average of computed potential energy surfaces for water−H_2 compared with the present experimental potential: (a) from ref 9, (b) from ref 10, and (c) from ref 11.

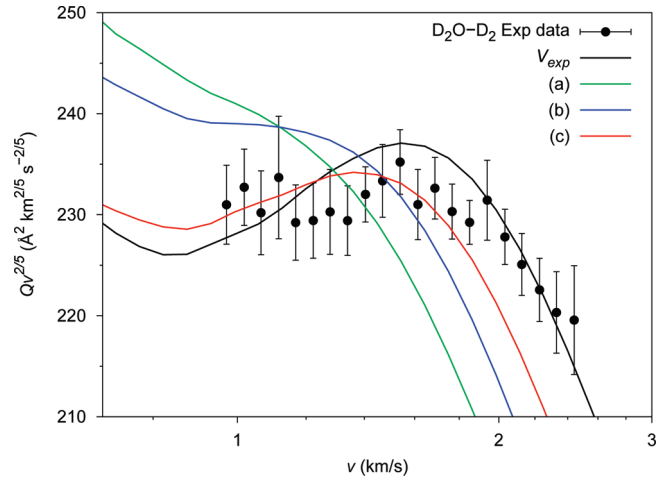

Figure 5. Theoretical cross-section profiles for water−H_2 obtained from the radial potentials in Figure 4 compared with the experimental results: (a) from ref 9, (b) from ref 10, and (c) from ref 11.

transfer (CT), we show how the presence of even a small amount of CT can be reliably ascertained, and we finally discuss a simple model to estimate the energy contribution associated with CT and how this compares with the experimental findings.

Before turning to this theoretical and computational analysis of CT effects, we note that the $Q(v)$ data measured for D_2O-D_2, enabling the determination of the radial part of the intermolecular potential, also provide a direct test of the accuracy of calculated PESs for the system. We have calculated the spherical average of three recent PESs for H_2O-H_2,[9−11] and the radial curves obtained are compared with the experimental determination in Figure 4. The corresponding ε and r_m parameters are reported in Table 1. Note that the isotropic average is by definition the first angular term (within a normalization factor) of the angular expansion employed by Phillips et al.[9] and Valiron et al.[11] In order to make the comparison with experiment more stringent, we evaluated, from the flexible PES of ref 11, the spherical average for the isotopologue D_2O-D_2, in addition to H_2O-H_2. The two differ negligibly (see Table 1), and only one is displayed in the figure. These isotropic potentials were then used to calculate theoretical cross-section curves to be compared with the experimental data. These are shown in Figure 5. Both this figure and Figure 4 clearly show that the PES reported by Valiron et al.[11] is of superior quality and in substantial better agreement with the experiment as compared to the previous calculations. It appears to underestimate the average binding energy by less than 1 meV ($\sim$8 cm^{-1}), which is well within the combined error bounds of experiment and calculations.[11] Let us recall here that the full-dimensional H_2O-H_2 PES described by Valiron et al.[11] was obtained by combining standard CCSD(T) calculations with elaborate, explicitly correlated CCSD(T)-R12 calculations. The latter calculations are expected to provide an accuracy of a few cm^{-1}, close to the basis set limit, as further discussed below. We note that, in the present work, a proper rigid-rotor D_2O-D_2 PES was obtained from the flexible H_2O-H_2 PES by accounting for both the different monomer-averaged geometries and the shift of the D_2O c.m. with respect to H_2O. Details on the coordinate transformation will be presented in a forthcoming paper,[16] together with a discussion of the impact of such isotopic effects on the scattering dynamics. The present results suggest, however, that the isotropic average of both PESs are very similar and that the isotopic effects are essentially negligible here (see Table 1).

Theoretical Calculations: Charge Displacement Analysis. As we have seen, the average binding energy between water and H_2 exceeds that which would result from vdW and induction forces by not more than 2 meV (see Figure 3 and Table 1). Where does this small but precisely measured effect originate, and what role does it play in governing the interaction? Tracing the origin of such small effects is a challenge. A quantitative description of these weak intermolecular interactions requires the use of theoretical methods that describe electron correlation accurately and large basis sets. The suggestion emerging from the experimental results, that the small stabilization observed may originate from a CT component in the interaction (this is, in fact, the only component that it is missing in the model), is also difficult to prove or refute *a priori*. If present, this CT may not be much larger than a few millielectrons (me) and therefore would be difficult to ascertain, but, indeed, a non-negligible energy contribution may be associated with it.[28] This is not the first time that such a situation has been encountered: recently we studied CT phenomena in the interaction between water and the series of noble gases (Ng). By quantitatively correlating theoretical results and experimental observations, it was possible to prove for the first time that a small CT (of the order of a couple of millielectrons) takes place from the Ng to water.[17,18] Furthermore, it was found that this CT is a strongly stereoselective, anisotropic phenomenon that is mediated by an asymmetric donor−acceptor concerted role of the two hydrogen atoms of the water molecule, which can in fact dictate the equilibrium geometry of the adducts.[17,18] The water−H_2 interaction energy surface is clearly much more anisotropic than that of water−Ng. Do CT effects play a role in this?

The key approach in our analysis is the study of the electron density changes taking place upon formation of the water adducts. The electron density change ($\Delta\rho$) is defined as the density difference between the complex and the isolated non-interacting partners placed at the same positions they have in the adducts.[29] But how do we define and measure CT? In principle, this simply cannot be done without resorting to some charge decomposition model, which may leave room to doubts

(28) Khaliullin, R.; Bell, A.; Head-Gordon, M. *Chem.−Eur. J.* **2009**, *15*, 851–855.
(29) Note that this definition includes the change in density due to the antisymmetrization and renormalization of the total wavefunction made up from the non-orthogonal fragment wavefunctions.

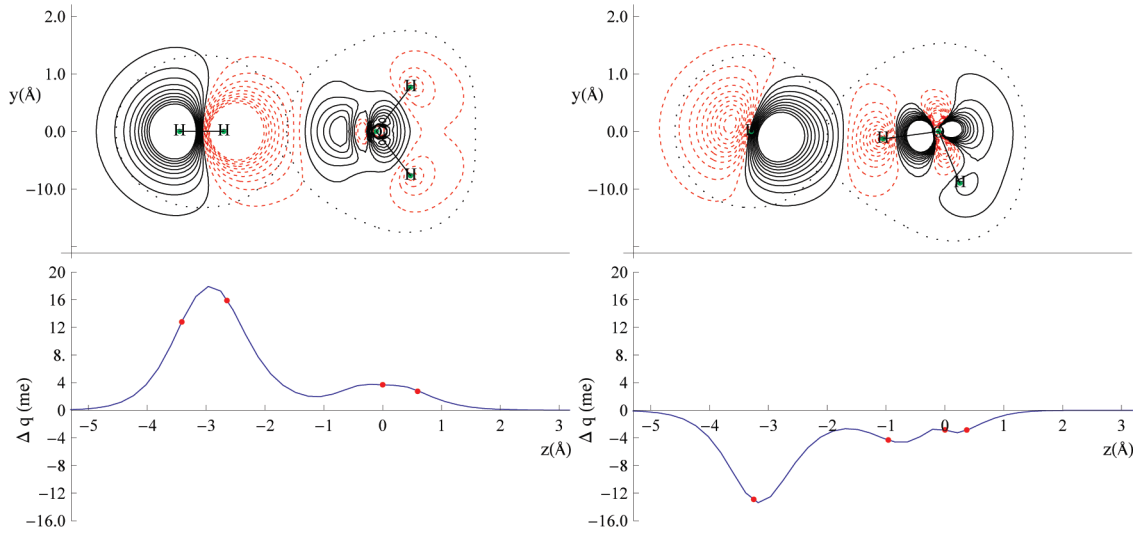

Figure 6. Contour plots of the electron density changes (upper) and CD curves (lower) for the H_2O-H_2 complex in the absolute (left) and secondary (right) minima configurations. In the contour plots, the red lines (dashed) denote negative values (density depletion), and the black lines (solid) are positive contours. The dotted contours mark the tangent isodensity levels of the isolated fragments. The circles on the Δq curves mark the projection of the nuclear positions on the interfragment axis z (joining the centers-of-mass of water and hydrogen). The axis origin is at the oxygen position. See the text for more details.

and provide a too narrow perspective, especially in cases where CT is very small. To free our results from any particular theory of charge decomposition, we adopt a scheme based on the definition of charge displacement (CD) along a given direction (z), given by

$$\Delta q(z) = \int_{-\infty}^{\infty} dx \int_{-\infty}^{\infty} dy \int_{-\infty}^{z} \Delta\rho(x, y, z')\, dz' \qquad (3)$$

where $\Delta\rho$ is the electron density difference as defined above. $\Delta q(z)$ measures, at each point z along the chosen axis, the electron charge that, upon formation of the adduct, is transferred from the right to the left side of the perpendicular plane through z.[30] (A negative value thus corresponds to electron flow from left to right.) In the water$-H_2$ system, z is chosen as the line joining the c.m. of H_2 and the c.m. of the water molecule. The charge displacement thus defined gives a picture of the direction and extent of electron transfer over the whole interfragment space, free of any scheme. This still leaves open the question of how to define the exact amount of CT taking place, but, as we shall see in the following and have already discussed,[17] the broad perspective offered by the CD curves, eq 3, makes, in the case at hand, a precise answer to this question almost totally irrelevant. The electronic density considered in the following was obtained in all cases at the coupled-cluster level of theory[31] with single and double excitations (CCSD) using the aug-cc-pVQZ basis set.[32] The calculations were performed with the program MOLPRO.[33] With the basis set used, the CD curves are very well converged. We recently presented a detailed study of the basis set dependence of the CD curves for a related system.[17] In studying their interaction, water and hydrogen were considered as rigid rotors, with geometries that correspond to the average of the ground vibrational states of the isolated molecules, as was done by Hodges et al.[10] and validated by Valiron et al.[11] We use the conventions reported in this previous work in defining the H_2O-H_2 rigid-rotor coordinate system. The intermolecular arrangement has been expressed as a function of five coordinates, namely, the intermolecular distance r from the c.m. of H_2O to the c.m. of H_2, and two pairs of relative angles (θ,ϕ) and (θ',ϕ') that describe, respectively, the collision direction and the orientation of H_2 relative to the H_2O body-fixed system. The main features of the PES, as recently reported by Valiron et al.,[11] are as follows. In the most stable configuration of the complex, where $\theta = \theta' = 0$ and $r = 3.08$ Å, the H_2 molecule lies on the C_2 axis of water on the oxygen side. The corresponding interaction energy is 29.1 meV (235.14 cm^{-1}). These values agree with the best calculations reported by Hodges et al.[10] A secondary minimum of the PES is located at $r = 3.21$ Å, with $\theta = 119°$ and $\theta' = 90°$. Thus, in this configuration, H_2 lies perpendicular to the water's plane and its c.m. is located on the plane, close to the axis of an O$-$H bond of water on the H side. In this configuration, the interaction energy is 24.7 meV.[11] For consistency, we have reoptimized these equilibrium structures at the same CCSD/aug-cc-pVQZ level of theory used to obtain the electron densities. The geometries obtained differ by less than 0.03 Å, and the BSSE-corrected interaction energies differ by less than 4 meV.

Charge Transfer at the Equilibrium Geometries. We start our analysis of the water$-$hydrogen molecule interaction at the geometry of the two minima of the PES. The upper panels in Figure 6 show the contour plots of the electron density difference for the absolute and the secondary minima. The dotted contours mark the isodensity levels of the isolated fragments that are equal in value and tangent, and they may thus be taken as a plausible representation of boundaries enclosing the non-interacting fragments. The lower panels in Figure 6 report, on the same horizontal scale as the upper plots, the corresponding Δq curves (eq 3). The density deformation contour plot for the absolute energy minimum (on the left) shows that the H_2 electron cloud is strongly polarized by water's dipole, with a density depletion lobe around the hydrogen atom pointing toward

(30) Belpassi, L.; Infante, I.; Tarantelli, F.; Visscher, L. *J. Am. Chem. Soc.* **2008**, *130*, 1048–1060.
(31) (a) Raghavachari, K.; Trucks, G. W.; Pople, J. A.; Head-Gordon, M. *Chem* **1989**, *157*, 479–483. (b) Hampel, C.; Peterson, K. A.; Werner, H.-J. *Chem. Phys. Lett.* **1992**, *190*, 1–12.
(32) (a) Dunning, T. H. *J. Chem. Phys.* **1989**, *90*, 1007–1023. (b) Kendall, R. A.; Dunning, T. H.; Harrison, R. J. *J. Chem. Phys.* **1992**, *96*, 6796–6806.
(33) Werner, H.-J.; Knowles, P. J.; Lindh, R.; Manby, F. R.; Schütz, M.; et al. *MOLPRO*, version 2008.1, a package of ab initio programs; 2008; http://www.molpro.net.

oxygen (the "near" hydrogen) and a density accumulation lobe at the far hydrogen. Note that the depletion lobe extends in the region between the fragments and appreciably crosses their tangent isodensity boundary. A significant charge rearrangement takes place also in the water region, with a visible density depletion around the hydrogen atoms and accumulation around oxygen. It is remarkable how the density perturbation reaches deep into the inner region around the oxygen nucleus. Turning now to the corresponding CD curve, we note first that it is positive everywhere, which unambiguously indicates that there is everywhere CT in the direction going from water toward the hydrogen molecule. On the left, the pronounced polarization of the hydrogen molecule is evident from the shape of the curve around the position of the hydrogen atoms: it increases around the far hydrogen, indicating charge accumulation, reaches a maximum close to the midpoint between the hydrogens, and then decreases, reflecting the depletion lobe at the near hydrogen. The curve shows some amount of electron polarization also around water but remains positive everywhere between the two fragments, indicating a net CT from water to hydrogen.[34] The CD curve is relatively flat in a wide interfragment region, so that an actual single numeric value of CT one may take for reference would not be very much dependent on the definition of a boundary point. About 1.14 Å from oxygen, the CD curve presents a minimum of 1.95 me, which may thus be taken as a lower limit for CT. At the isodensity boundary between the fragments defined above (about 1.55 Å from oxygen), the amount of CT is 2.85 me. The amount of charge transferred to the left does not vary much across the whole water region; at the position of the water's hydrogen atoms, CT is the same 2.85 me found at the isodensity boundary. It is remarkable that CD to the left begins on the right side of water's hydrogens and, with long-range effect, reaches, uninterrupted, the far hydrogen of H_2.

Very remarkably, the picture of CD that emerges for the nuclear configuration corresponding to the secondary minimum is completely opposite (right panels of Figure 6). H_2 polarization is still pronounced but in the opposite direction, with electron depletion taking place away from water and accumulation toward water. It is this lobe of density increase that now extends between the fragments and crosses their boundary. A significant charge rearrangement again also takes place in the water region, and, quite surprisingly, there is a visible density depletion around the hydrogen atom closer to the approaching hydrogen molecule. This is accompanied by a polarization of the oxygen site that extends to the far hydrogen. As a result, there is a charge accumulation in the region of both OH bonds. The corresponding CD curve immediately makes the characterization of the H_2O-H_2 interaction in this configuration even clearer: it is eye-catching that the function here is *negative* everywhere. Thus, everywhere in the complex there is a net CD from left to right, i.e., in the direction going from the hydrogen molecule toward water. Electrons flow away from the left side of the H_2 molecule until a minimum is reached, remarkably close to the projection on the z axis of the nuclear positions. After this minimum, the CD curve starts to reaccumulate rapidly until about 1.8 Å from oxygen, where a maximum is found (minimum CT magnitude). The value of CT at this point is 2.67 me. The value at the isodensity boundary between the fragments is 3.08 me. This amount does not vary much going toward water, at least up to the position of the near hydrogen, which corresponds almost exactly to a shallow minimum. Note that, quite surprisingly, appreciable CT can still be seen, even in the region of the far hydrogen atom. But here, in contrast to the region around the left hydrogen, the positive slope of the curve indicates that this hydrogen is an electron acceptor. At the nuclear position of this hydrogen, the CD curve is still negative, with 2.86 me being displaced from left to right. This asymmetric, concerted role of water's hydrogen atoms in mediating CT[17] may be an important peculiarity of general relevance in water's interactions. Overall, the CD pattern at the secondary minimum of the water$-H_2$ interaction is very similar to what we found for the water$-$Ng series.[17] We will discuss this analogy in greater detail later in this work.

(34) Note, by contrast, that the Δq curve goes to zero in the region between the fragments in the case of a pure vdW interaction (see, e.g., ref 17).

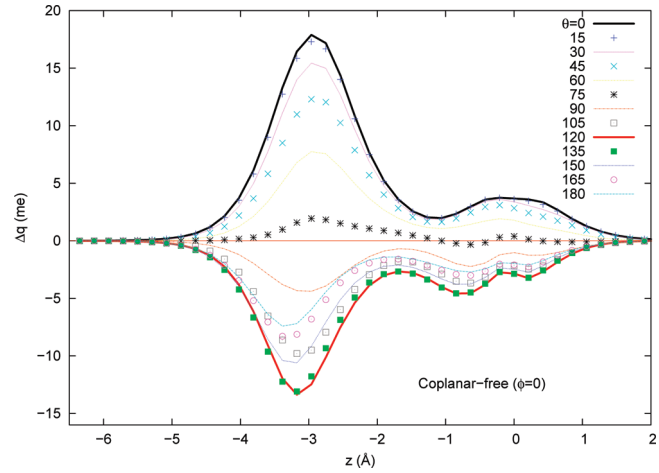

Figure 7. CD curves for different orientations of the H_2O-H_2 complex in the *coplanar-free* arrangement (see text). θ is the angle (in degrees) between the z axis (joining the c.m. of the fragments) and water's C_2 axis. $\theta = 0°$ corresponds to the global minimum configuration, while $\theta \simeq 120°$ corresponds to the secondary minimum.

Stereoselectivity of Charge Transfer. We have thus seen that the two minima of the potential energy of interaction between water and hydrogen are characterized by opposite patterns of CT, with water being an electron donor at one geometry and an electron acceptor at the other. At this point, an interesting question is how the occurrence and extent of CT are generally correlated with the geometry of the water$-H_2$ complex and the anisotropy of its electronic energy surface. For this purpose we have calculated the CD curves for H_2O-H_2 in different intermolecular arrangements, and we analyze the results in the following.

The first interesting section of the PES to consider is that corresponding to the hydrogen molecule circling around water with its c.m. kept on the water plane. In other words, we consider the section characterized by $\phi = 0$, obtained by varying the angle of approach θ. At each fixed θ value, the other coordinates, r, θ', and ϕ', are reoptimized. We call this particular minimum energy walk *coplanar-free*. Note that it includes the nuclear configuration of the two main minima of the global PES; therefore, it encompasses a transition from $H_2O \rightarrow H_2$ CT to the opposite situation. The computed CD curves at various values of θ, from 0° to 180° in steps of 15°, are displayed in Figure 7. $\theta = 0°$ corresponds to the global minimum and $\theta = 180°$ to a constrained maximum (saddle point), where the H_2 axis lies perpendicular to the water plane. The whole walk is contained in an energy interval of only about 13 meV (100 cm^{-1}), but, as Figure 7 clearly shows, the CD curves vary significantly along it, displaying a strong anisotropy with the angle of approach.

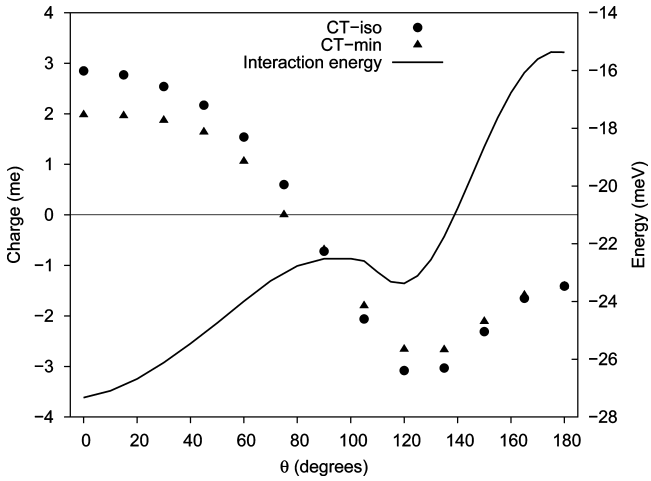

Figure 8. CT evaluated at the isodensity boundary (CT-iso) and at the minimum magnitude (CT-min) of the CD curves for different orientations of the H_2O-H_2 complex along the *coplanar-free* PES cut (see text). The corresponding interaction energy curve is also shown. Positive CT is from water to H_2, negative from H_2 to water. θ is the angle between the line joining the center of mass of the fragments and water's C_2 axis, with $\theta = 0°$ corresponding to the global energy minimum and $\theta \simeq 120°$ to the secondary minimum.

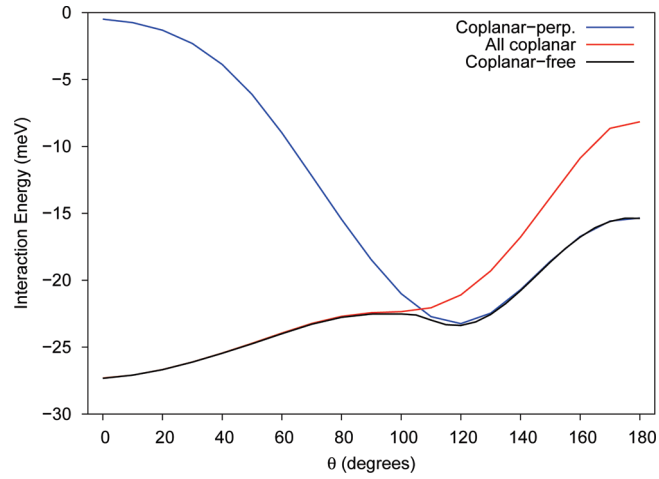

Figure 9. Energy profile along the coplanar-free, coplanar-perpendicular, and all-coplanar paths of revolution of H_2 around water (see text). θ is the angle between the line joining the center-of-mass of the fragments and water's C_2 axis. $\theta = 0°$ corresponds to the global energy minimum, while $\theta \simeq 120°$ corresponds to the secondary minimum.

The most interesting finding is that the CD curves corresponding to the two minima on the PES ($\theta = 0°$ and $\theta \simeq 120°$) are the most positive and the most negative, respectively, defining a boundary enclosing all the others. Although other contributions to the interaction energy may be maximal at the two stable geometries, and in particular at the absolute minimum,[10] it would be difficult to ignore the evident suggestion that CT is a crucial stabilization factor.

The clear correlation between CT and the profile of the cut of the PES is well illustrated in Figure 8. Here we report, together with the computed energy profile along the coplanar-free path, the corresponding plot of two different CT estimates extracted from the CD curves. One estimate is taken at the isodensity boundary between the fragments defined earlier, and the other is taken at the point of minimum CD magnitude between the fragments. (Note that each CD curve exhibits just one such minimum in the whole interval between the c.m. of water and that of H_2.) These are just two easily defined reference points along a CD curve, but our reasoning would not be altered in the least by the choice of any other plausible boundary between the fragments. The global minimum configuration ($\theta = 0$), as we mentioned above, actually corresponds to the maximum of CT from water to the hydrogen molecule. Upon increasing θ from this point, CT decreases as the interaction energy also decreases, until CT goes to zero (for $\theta \simeq 80°$). For small angles of revolution θ, H_2 lies on the water plane, and its axis keeps pointing approximately toward the oxygen atom. It may be interesting to note that, if H_2 here is rotated out of the plane to a perpendicular position, the energy surface becomes repulsive (because of the dipole−quadrupole electrostatic effect) and CT vanishes. As θ increases further along the coplanar-free path, H_2 slowly rotates, at first remaining in the water's plane. In correspondence with the point of vanishing CT ($\theta \simeq 80°$), its axis lies roughly parallel to an OH bond, so that no hydrogen atom, either of water or of H_2, functions as an electron donor/acceptor. As θ increases above 80°, CT changes sign, and water becomes the electron acceptor. In the range 90−105°, the PES cut presents a local maximum; interestingly, in this region the CT curve presents a flex and changes its curvature. This region corresponds to a significant change in the nuclear arrangement in that, quite suddenly, H_2 rotates out of the water's plane and orients itself perpendicularly to it. It remains in the perpendicular orientation thereafter up to $\theta = 180°$. The secondary minimum configuration (at $\theta \simeq 120°$) coincides again with a CT maximum, this time from H_2 toward water. As we move further from the secondary minimum toward still larger θ values, CT decreases again, and the complex is destabilized, until the energy reaches a saddle point at $\theta = 180°$. These findings show the existence of a strict correlation between charge-transfer phenomena and the interaction energy in these weakly bound adducts.

The rapid change in H_2 orientation, from coplanar to perpendicular to water for $\theta \simeq 105°$, is interesting and can be seen clearly in Figure 9, which shows the computed energy profile along three paths on the CCSD/aug-cc-pVQZ PES. One corresponds to H_2 being constrained to remain perpendicular to the water plane as it circles around it (*coplanar-perpendicular* path). The second corresponds to H_2 constrained to remain on the water plane (*all-coplanar*), and the third is the *coplanar-free* path, which may thus clearly be viewed as the result of an avoided crossing between the former two paths.

We have also calculated the CD curves for an out-of-plane walk, where the hydrogen molecule circles around water with its c.m. lying in the σ_v plane of water ($\phi = 90°$). Again, also along this path all the other variables have been reoptimized for each value of the angle of revolution. The CT-iso and CT-min values obtained along the walk, together with the energy profile, are shown in Figure 10. Note that the point $\theta = 0°$ again coincides with the global PES minimum, as before, while $\theta = 180°$ again coincides with the saddle point of the *coplanar-free* surface. Along the present path, $\theta = 180°$ is a local minimum. Thus, a strict correlation between the energy profile and CT can be observed also in this case. In particular, the two points that correspond to the energy minima coincide with CT maxima in one direction or the other. Water is the electron donor (positive CT) from $\theta = 0°$ to $\theta \simeq 120°$, when CT vanishes. At larger θ values, water becomes the electron acceptor and CT increases monotonically to $\theta = 180°$. It is interesting to note that, compared with the coplanar path, the arc of H_2 revolution

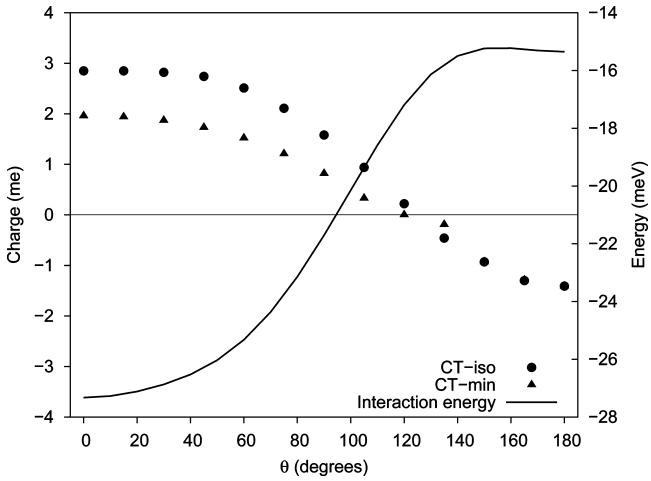

Figure 10. CT evaluated at the isodensity boundary (CT-iso) and at the minimum magnitude (CT-min) of the CD curves along the σ_v path (see text). The corresponding interaction energy curve is also shown. Positive CT is from water to H_2, negative from H_2 to water. θ is the angle between the line joining the center-of-mass of the fragments and water's C_2 axis, with $\theta = 0°$ corresponding to the global energy minimum.

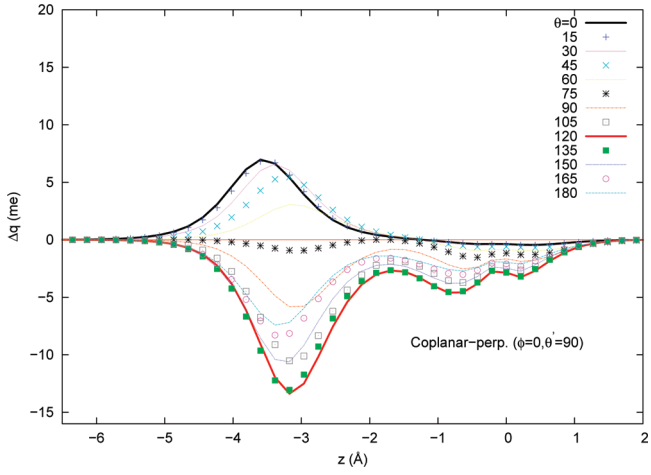

Figure 11. CD curves for different orientations of the H_2O-H_2 complex in a configuration with the center-of-mass of H_2 on water's plane and its molecular axis perpendicular to the water plane ($\theta' = 90°$). θ is the angle between the line joining the center-of-mass of the fragments and water's C_2 axis ($\theta = 0°$ on the oxygen side).

around water, in which the latter acts as the electron donor, is here about 40° wider.

Finally, it is further enlightening to examine briefly the CD patterns along a third potential energy section, corresponding to H_2 going around water with its c.m. on water's plane but with its axis constrained to stay perpendicular to the plane. These CD curves are shown in Figure 11. As we have seen, this cut essentially coincides with the coplanar-free one for θ larger than about 105° (see Figure 9). However, for θ smaller than about 75°, the CD curves exhibit a clearly different character than those of the unconstrained path, in that they essentially go to zero in the interfragment region and no appreciable CT takes place. This pattern, essentially consisting of charge polarization within the interacting fragments, is that characteristic of pure vdW interactions.[17] The angular dependence of the CD curves is in fact remarkably similar to the one we have found for the water−Ar system.[17]

In summary, the water−H_2 complex is characterized by a small but important CT effect. It is strongly stereospecific, and the two minima of the PES are characterized by the largest CT magnitudes, in opposite directions. The orientations in which the H_2 molecule approaches from the side of oxygen with its axis pointing toward O lead to CT from the water to the hydrogen molecule, which thus acts as an electron acceptor (proton donor). The orientations in which the H_2 molecule approaches from the side of water's hydrogen atoms also lead to a CT but of opposite sign, this being also maximal when H_2 approaches along the O−H direction or thereabout (secondary minimum of the PES). In this last case water acts as an electron acceptor (proton donor) toward H_2. In general, when H_2 approaches water with its axis perpendicular to water's plane, the interaction potential and the CT pattern are very similar to those observed and computed for the water−Ar complex. The existence of a clear correlation between CT magnitude and strength of the water−H_2 interaction suggests that CT may play a significant role in determining the marked anisotropy of the PES and the short-range reinforcement of the water−H_2 interaction observed experimentally. Because of the rotational averaging taking place in the experiment and of the orientational dependence of CT, the effective CT impact on the scattering potential will be smaller than that which may be computed in ranges close to the equilibrium geometries. We shall try to correlate theory and experiment more quantitatively in the next section.

A Simple Model for Charge Transfer. In the previous sections we have shown that a complex bidirectional CT component is present in the water−H_2 interaction and that a clear correlation appears to exist between CT anisotropy and the water−H_2 PES anisotropy. Combined with the very accurate experimental determination of a non-vdW energy component in the rotationally averaged potential, which by the nature of the experimental conditions excludes anisotropic electrostatic interaction components due to static multipoles, this strongly suggests that CT may be at the origin of this stabilization. It would be very interesting to assess more quantitatively the plausibility and consequences of this claim. For this purpose, we investigate here a very simple model enabling us to associate an energy contribution with CT that can be directly compared with the experiment. This analysis, although rough and preliminary, may provide useful insights for the design of effective models for the accurate description of weak interactions, including hydrogen bonding.[35]

The high accuracy of the experimental determination of the absolute interaction energy and the related data analysis based on the ILJ model is a key aspect of our study, because it provides very reliable experimental information on the radial dependence of the interaction energy and of its deviation ΔV from the vdW (plus induction) model, as shown in Figure 3:

$$\Delta V(r) = V_{exp}(r) - (V_{vdW}(r) + V_{ind}(r)) \qquad (4)$$

We would like, therefore, to obtain an estimate of the radial dependence of CT, averaged over all possible relative orientations of the colliding molecules, and examine how this may be related to the above experimentally determined r-dependent potential.

We begin by investigating the r-dependence of CT in two representative geometrical arrangements of the water−H_2 complex where we know that CT is large and of opposite sign, which

(35) For the official IUPAC project aimed at categorizing hydrogen-bonding and other intermolecular interactions, see http://www.iupac.org/web/ins/2004-026-2-100.

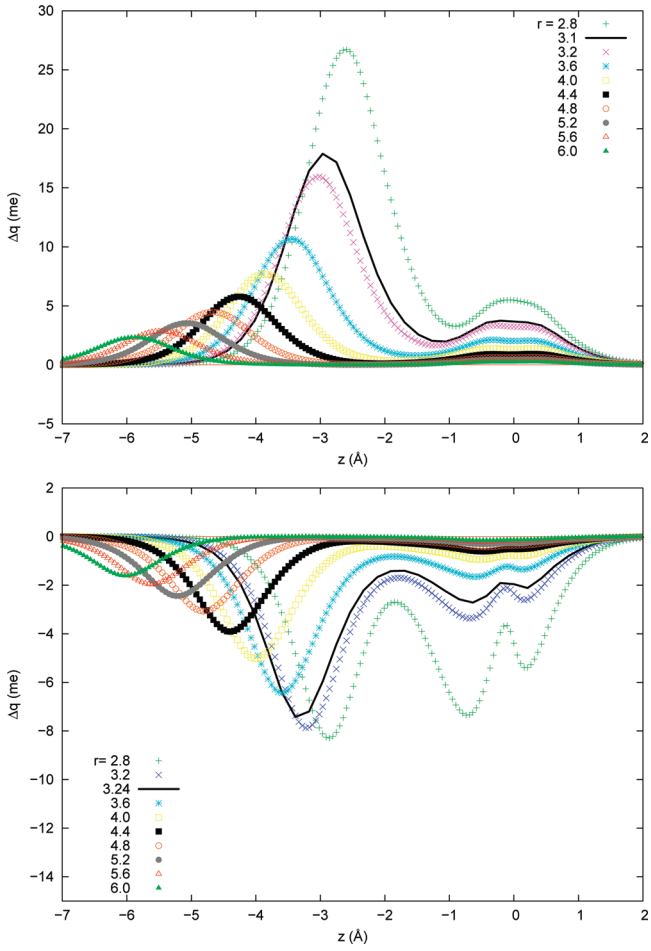

Figure 12. CD curves for different distances (r) between H_2 and water. In the upper panel, hydrogen lies on water's C_2 axis on the oxygen side ($\theta = 0$). $r = 3.1$ Å corresponds to the global PES minimum. In the lower panel, H_2 approaches water from the opposite direction ($\theta = 180°$), with its axis perpendicular to water's plane. Here, $r_m = 3.24$ Å corresponds to the energy minimum along the path.

correspond to the most stable configurations for $\theta = 0°$ and $\theta = 180°$, respectively. In the first orientation, H_2 approaches water from the oxygen side, along the C_2 axis. Along this path lies the absolute minimum of the PES, and water→H_2 CT is maximal, as discussed earlier. In the second configuration, H_2 is the electron donor and approaches water from the opposite direction, with its bond axis perpendicular to the water's plane and its c.m. on it. The CD curves obtained for the two configurations at various r values in the range 3.2−6.0 Å are shown in Figure 12. Clearly, the curve amplitudes decrease with increasing distance. The magnitude of CT taken at any given point between the fragments along the curves decreases exponentially with distance. Perhaps surprisingly, however, CT shows a very similar decay behavior in both of the orientations examined. For the sake of definiteness, we consider the CT magnitude at its minimum between the fragments, but essentially identical results are obtained by taking CT at the isodensity boundary defined earlier. The resulting r-dependence of CT is shown in Figure 13. The nearly identical behavior in two configurations characterized by very different density redistributions and charge flowing in opposite directions is remarkable and, at least for the present, very preliminary discussion, justifies making the simplest approximation, namely that the r-dependence of CT is the same regardless of the relative orientation

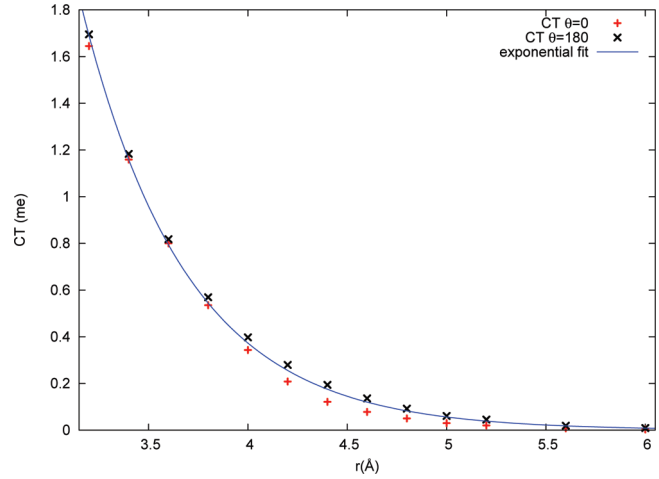

Figure 13. Dependence of CT on the distance r between the center-of-mass of H_2 and water for the two configurations of Figure 12. The exponential curve shown is the mean of the best-fit curves for the two sets of data.

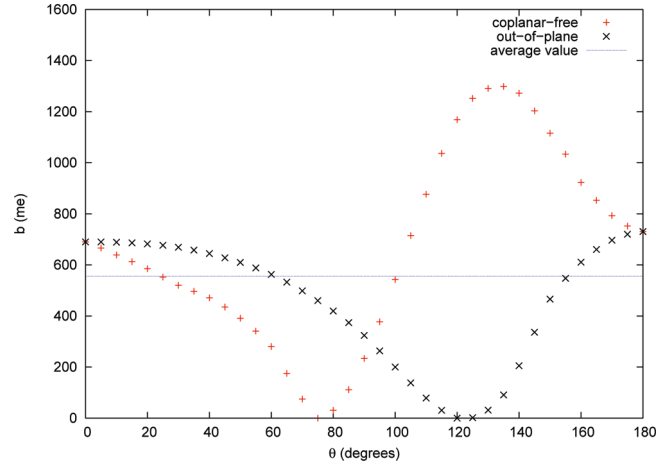

Figure 14. Value of the parameter $b(\theta, \phi)$ in eq 5 along the coplanar-free and out-of-plane PES cuts (see text). The average value of the data shown is indicated by a horizontal line.

of the fragments. Further omitting any dependence from the orientation of the H_2 axis, we thus write

$$\mathrm{CT}(r, \theta, \phi) = b(\theta, \phi)\, \mathrm{e}^{-ar} \qquad (5)$$

and henceforth we take for a the value of 1.89 Å^{-1}, which is the mean of the values obtained by fitting the two sets of data in Figure 13 (1.81 and 1.97 Å^{-1}).

In order to make a comparison with the experiment, we should now obtain at least a rough estimate of the average value of the prefactor b over all possible relative orientations of water and H_2. Information on the angular dependence of b can be easily gained from the computed values of CT at any geometry. As an example, we show in Figure 14 the variation of b along the PES cuts discussed earlier, the *coplanar-free* and *out-of-plane* walks of Figures 8 and 10. If we now simply consider these two walks as roughly representative samples of all the possible relative orientations of the two fragments, we may take the average of b over the displayed values to express the sought spherically averaged CT:

$$\mathrm{CT}(r) = \bar{b}\, \mathrm{e}^{-ar} \qquad (6)$$

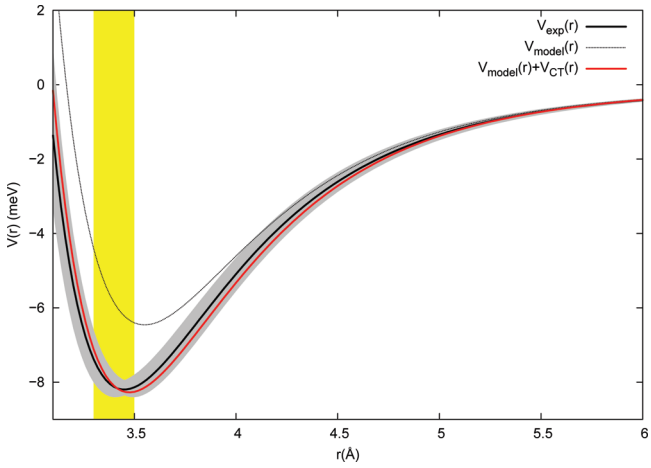

Figure 15. Isotropic interaction energy for H_2−water. V_{exp} is the experimental determination, $V_{model} = V_{vdW} + V_{ind}$ (see Figure 3), and V_{CT} is given by eqs 6 and 7, with $k = 2.5$ eV/e. The gray region shows the experimental uncertainty on V_{exp} (see the caption of Table 1), and the yellow band marks the r range most sensitively probed by the experiment.

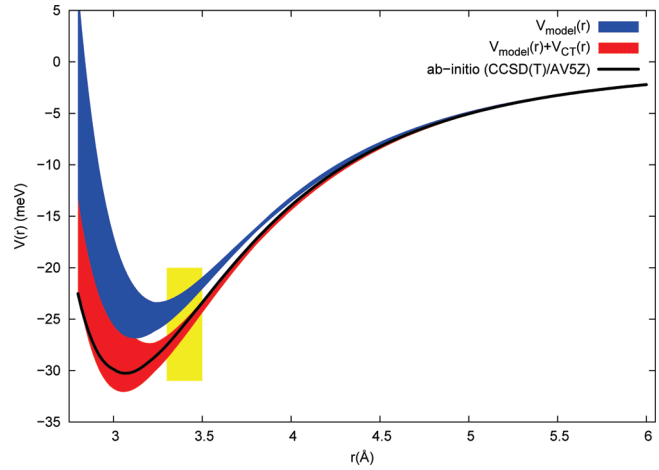

Figure 16. Comparison of a model potential for H_2O−H_2 in a specific orientation (see text) with CCSD(T)/aug-cc-pV5Z calculations, as a function of the interfragment distance r. $V_{model} = V_{vdW} + V_{ind} + V_{elec}$ (eq 8). V_{CT} is given by eqs 6 and 7. The colored bands illustrate the spread in the model potential resulting from a change of ±3% in the parameters that define it (see the Supporting Information). The yellow band shows the r range most sensitively probed by the scattering experiments.

where the average $\bar{b} = 556$ me is indicated in the figure by a horizontal line. We now simply assume that the energy contribution associated with this CT is approximately proportional to it,[28,36]

$$V_{CT}(r) = k\,\mathrm{CT}(r) \tag{7}$$

and see if this formula, with the sole unknown parameter k, the energy per transferred unit charge, can provide a reasonable representation of the experimental measurements. The fit of the experimental $\Delta V(r)$, eq 4, yields $k = 2.5$ eV per electron and is shown in Figure 15. Given the simplicity of the model adopted, the accuracy of the fit over the entire r range considered is remarkable. The model provides $r_m = 3.48$ Å and $\varepsilon = 8.3$ meV, in excellent agreement with the experimentally determined values (see Table 1). One cannot fail to notice the telling circumstance that, although the ILJ potential form contains no exponential terms, the observed *stabilization energy*, eq 4, is accurately described by an exponential.

The above analysis appears to support quite strongly the conclusion that the entire difference between the experimentally measured isotropic interaction potential and that described by vdW plus induction forces is due to CT. We emphasize again that, in the given experimental conditions, the colliding molecules are rotationally hot, and therefore all electrostatic contributions (largely due at long-range to the interaction between water's dipole and hydrogen's quadrupole) are averaged out and do not contribute. Our analysis also makes the implicit assumption that the CT energy contribution is additively separable from the rest. This is justified in the r range probed by the experiment (and at longer distances), in view of the weakness of the interaction and the small charge transferred.

We can make a further independent verification of the soundness of the value of the crucial quantity k, the energy per transferred electron, provided by the fit discussed above. In a specific geometric arrangement of the water−H_2 complex where, in contrast to the rotationally averaged situation of the experiment, electrostatic contributions to the potential play a dominant role, we can estimate the interaction energy using a model that includes $V_{CT}(r)$ as determined above and compare this with accurate ab initio results. We choose the $\theta = 0$ path going through the absolute PES minimum, where H_2 lies along water's C_2 axis on the oxygen side, with r varying in the range 2.8−6.0 Å. For this configuration we have performed additional accurate energy calculations at the CCSD(T) level,[31,37] which includes perturbatively estimated triple-excitation contributions, with the larger aug-cc-pV5Z (AV5Z) basis set.[32] At this level of theory, the BSSE-corrected interaction energy is 29.4 meV, essentially coincident with that of ref 11. The model potential we use can be written

$$V(r) = V_{vdW}(r) + V_{ind}(r) + V_{elec}(r) + V_{CT}(r) \tag{8}$$

where V_{vdW} is the vdW term (comprising size repulsion and dispersion attraction) and V_{ind} is the induction term (depending on hydrogen's parallel polarizability and water's dipole). V_{elec} is the electrostatic contribution, which, for the configuration of interest here ($\theta = 0$) and at intermediate and large intermolecular distances, can be properly described by the first term of the multipole expansion (i.e., the classical dipole−quadrupole term). V_{vdW} is a recently proposed model[38] in which the interaction with water is represented as a sum of three contributions associated with polarizability ellipsoids representing, respectively, oxygen and the two OH bonds. All details of the model potential can be found in the Supporting Information. In the computation of $V_{CT}(r) = k\,\mathrm{CT}(r)$, we used $k = 2.5$ eV/e, as determined above, and the CT values corresponding to the minimum magnitude in the interfragment region of the CCSD(T)/aug-cc-pV5Z CD curves. The results of these calculations are displayed in Figure 16, where we show separately the curves corresponding to the model potential with (red) and without (blue) the inclusion of the CT term. The potentials are represented as colored bands in order to account for a reasonable degree of

(36) Reed, A. E.; Curtiss, L. A.; Weinhold, F. *Chem. Rev.* **1988**, *88*, 899–926.
(37) Deegan, M. J. O.; Knowles, P. J. *Chem. Phys. Lett.* **1994**, *227*, 321–326.
(38) Albertí, M.; Aguilar, A.; Cappelletti, D.; Laganà, A.; Pirani, F. *Int. J. Mass Spectrom.* **2009**, *280*, 50–56.

variability (±3%) in the four parameters governing the V_{vdW} interaction component (see the Supporting Information). The figure makes evident that the inclusion of the V_{CT} term described earlier, with the constant k derived by comparison with the experiment, not only affects the potential in significant proportion at all distances shorter than about 4.5 Å but also, crucially, brings the model in near-quantitative agreement with the accurate ab initio potential. This conclusion is largely independent of the details of the description of the vdW interaction; note how the variation in the V_{vdW} component affects the potential significantly only in the regions of the minimum and of the repulsive wall, but only marginally at intermediate and longer distances (and, in particular, in the range most sensitively probed by our experiments), where CT effects remain, instead, crucially relevant. At very short range, the uncertainties in the model equal or exceed the energy stabilization due to CT, and the simple additive form of the potential we have assumed may itself break down.

In conclusion, this simple analysis is fully consistent with, and strongly supports, our estimate of the energy contribution associated with CT (about 2.5 eV per electron) and the additivity of the potential components at r larger than about 3.3 Å. This appears to be valid in situations both where the electrostatic component of the interaction is absent or largely averaged out and where it is dominant. Note that, in the $\theta = 0°$ arrangement just examined, at a distance $r = 3.45$ Å, corresponding to the minimum of the experimentally measured potential, the electrostatic term represents about 49% of the total attractive component of the potential (32.5 meV), the dispersion term 35%, the CT energy 9%, and the induction term 7%. As we have argued above, we cannot very confidently adopt our simple additive model at much shorter distances. For reference, however, it may be useful to report that, at the absolute and secondary minima of the water−H_2 PES, we estimate that V_{CT} may be up to one-third of the total interaction energy. To our knowledge, this is the first time that the absolute scale of the energy stabilization due to CT is determined and rationalized on the basis of experimental observations. In summary, all our results strongly suggest that, far from negligible, CT is an important driving force in governing the water−H_2 interaction, its anisotropy, and the spatial arrangement of the complex. Finally, it is interesting to note that the present findings place the bond stabilization by CT on the same scale as the effects that have been characterized by scattering experiments on systems involving open-shell atoms (with high electron affinity) and closed-shell partners (noble gases and simple molecules).[39,40]

Concluding Remarks

The experimental data presented in this work are an important test of the absolute scale of the isotropic intermolecular interaction for the water−hydrogen system. We clearly demonstrate that only the most recent theoretical calculations provide a spherical component of the PES that describes with acceptable accuracy the experimentally observable $Q(v)$.

A detailed analysis of the experimental data obtained, using various approaches, shows beyond uncertainty that water and H_2 interact significantly more strongly (by as much as 30% of the spherically averaged binding energy measured by the scattering experiments) than would be expected considering vdW and induction forces (the electrostatic interaction between permanent multipoles is averaged out under the experimental conditions). This stabilization energy decays exponentially with distance and, with excellent approximation over a wide distance range, is found to vary linearly with the magnitude of CT calculated by accurate ab initio density calculations and the model-free approach provided by the CD analysis. We conclude that CT is responsible for the measured interaction strengthening, with a contribution of about 2.5 meV per millielectron transferred. A simple model based on the experimental measurements and the calculated CT is capable of predicting accurately, again over a wide distance range, the interaction energy computed by state-of the-art CCSD(T)/aug-cc-pV5Z calculations.

The calculations show that CT effects are extremely stereospecific and in fact suggest that CT is crucial in determining the PES anisotropy and the precise location of the energy minima, thus controlling also important dynamical properties such as rotational inelasticity. Very interestingly, CT flows in opposite directions at different complex geometries. When H_2 approaches water over a wide solid angle on the oxygen side, and in particular at the global PES minimum, water acts as an electron donor (proton acceptor) and the H_2 axis points toward oxygen. When H_2 approaches from the opposite region of space, including the secondary PES minimum, water is the electron acceptor and the H_2 axis tends to orient itself perpendicular to the water plane. In this situation, the CD pattern is very similar to that found in other water adducts,[17] with both OH bonds playing a concerted asymmetric role in redistributing the extra density.

Measurable CT effects have been recently demonstrated to take place also for the water−Ng complexes,[17] and therefore a comparison with the latter is important. For D_2O-D_2 the measured CT stabilization energy is similar to that observed for D_2O-Ar. Indeed, CT depends to a first approximation on the ionization potential I of the species involved, and $I_{H_2} \simeq I_{Ar}$. Interestingly, however, the vdW part of the interaction is much less for D_2O-D_2 than for D_2O-Ar, depending mainly on the polarizabilities ($\alpha_{Ar} \simeq 2\alpha_{H_2}$). Therefore, the relative CT stabilization is much larger for D_2O-D_2 and also has a larger effect on the experimental observable. Furthermore, since we measure an average effect, the CT contribution is larger for specific geometric arrangements (by a factor of 3 or 4).

The CT energy contribution determined for the H_2O-H_2 system is consistent with that calculated recently for other cases. A relevant reference case is that of the water dimer, for which the calculated CT energy[41] is 2−3 times larger than that estimated here for water−hydrogen, consistent with the much shorter intermolecular distance in $(H_2O)_2$. The specific energy associated with CT in the water dimer is also much larger.[28] It is, however, necessary to underline that, for $(H_2O)_2$, the intermolecular energy is dominated by dispersion and electrostatic forces, so CT plays a relatively minor role.[41] In contrast, for H_2O-H_2, but also for many other similar systems which we are investigating, where electrostatic energy is much less, CT is much more relevant and can constitute as much as 20−40% of the size repulsion.

(39) Pirani, F.; Giulivi, A.; Cappelletti, D.; Aquilanti, V. *Mol. Phys.* **2000**, *98*, 1749–1762.
(40) Pirani, F.; Maciel, G. S.; Cappelletti, D.; Aquilanti, V. *Int. Rev. Phys. Chem.* **2006**, *25*, 165–199.
(41) Stone, A. J.; Misquitta, A. J. *Chem. Phys. Lett.* **2009**, *473*, 201–205.

If the relevance and stereospecificity of CT are proved to be peculiar to weak intermolecular interactions involving water (for the water−methane adduct see, e.g., ref 42), the findings of the present work may constitute an important tessera in the mosaic of water's chemistry.

Acknowledgment. This work was supported by the Italian Ministero dell'Istruzione, Universita e Ricerca, through PRIN grant no. 2008KJX4SN_003. M.L.R. thanks the ACS-IREU programme for financial support through award no. CHE-0755206 from the U.S. National Science Foundation.

Supporting Information Available: Details of the model potential used; optimized geometries and corresponding energies of the calculated structures; complete refs 2a and 3. This material is available free of charge via the Internet at http://pubs.acs.org.

JA1056642

(42) Raghavendra, B.; Arunan, E. *Chem. Phys. Lett.* **2008**, *467*, 37–40.